hv photonics

IMPACT FACTOR 2.4

CITESCORE 2.3

Article

Manipulation of Population Levels through Zeno-Type Measurements

Javier Contreras Sánchez, Fray de Landa Castillo-Alvarado and José Luis Hernández-Pozos

MDPI

https://doi.org/10.3390/photonics10101170

photonics

MDPI

Article

Manipulation of Population Levels through Zeno-Type Measurements

Javier Contreras Sánchez [1], Fray de Landa Castillo-Alvarado [1] and José Luis Hernández-Pozos [2,*]

[1] Escuela Superior de Físico-Matemáticas, Instituto Politécnico Nacional, Mexico City 07738, Mexico; javcontreras@ipn.mx (J.C.S.); flcastillo@ipn.mx (F.d.L.C.-A.)
[2] Departamento de Física, Universidad Autónoma Metropolitana-Iztapalapa, Mexico City 09310, Mexico
* Correspondence: jlhp@xanum.uam.mx

Abstract: We present a scheme, based on Bloch equations and Zeno-type measurements, that allows the control of the probability density evolution of the eigenstates of a V-type system. The equations are solved numerically and we present how the population in each level can be controlled using different sequences of "pulse measurements". The entropy between the "measurement device" and the field used to perform the measurement process is evaluated for different strengths of such field, these calculations show that the entropy is maximized when we are in the Zeno regime. The results shown here unveil different possible strategies for controlling the population levels of a V-type system and could be implemented, for example, in trapped ions or RMN qubits.

Keywords: Zeno-type dynamics; quantum control; quantum measurement

1. Introduction

As the implementation of quantum technologies such as quantum communications and quantum computing is becoming a reality, the control of quantum systems is paramount to achieve more robust practical implementations.

We briefly recall that Misra & Sudarshan [1] showed theoretically, Cook proposed a feasible experiment [2] and Itano et al. [3] proved experimentally with trapped ions, that for a system with quadratic time decay dependence, rapid and successive measurements on the system have the effect of freezing its evolution. This is known as the quantum Zeno effect (QZE). It should be pointed out that several years before these developments, Khalfin [4] found the necessary condition for a non-exponential decay, which is necessary for the Zeno-type evolution.

As is well known, the effect of an instantaneous measurement is described by the Von Neumann's projection postulate, which states that the wavefunction describing the system is projected onto the eigenspace of the observable under measurement. In turn, the measurement destroys all the possible eigenstates. However, Pokorny et al. [5] have shown an experiment in which some superpositions may survive and propose their scheme as an ideal measurement of the ion–photon coupling.

In the Sudarshan and Itano papers cited before, the postulate of the "collapse of the wavefunction" caused by the measurement pulses is used for the interpretation of the results. However, it has been established by Frerich at al. [6] that it is not necessary to invoke such a postulate; the same results can be described if we consider the evolution of a "V"-type three-level system coupling the ground state to each of the upper levels via two electromagnetic fields and following the three levels and the evolution of the two e.m. fields using Bloch equations.

Similarly to the quantum Zeno effect (QZE), we can obtain the anti-Zeno (QAZ) effect: while the QZE is referred as the freezing of the system's evolution, the QAZ effect is the acceleration of the quantum evolution of a system due to frequent measurements [7–11]. Based on these two complementary effects, we can see that by carefully engineering the

Citation: Contreras Sanchez, J.; Castillo-Alvarado, F.d.L.; Hernández-Pozos, J.L. Manipulation of Population Levels through Zeno-Type Measurements. *Photonics* **2023**, *10*, 1170. https://doi.org/10.3390/photonics10101170

Received: 17 July 2023
Revised: 26 September 2023
Accepted: 4 October 2023
Published: 20 October 2023

interaction between the different parts of an atomic system interacting with electromagnetic fields, it is possible, within certain limits, to control its evolution.

Since the early experiment of Itano et al., there has been considerable interest in this field, with many theoretical and experimental works published. Here, we cite very few of them. For example, possible applications of quantum Zeno dynamics have been proposed, such as the error correction in quantum computers [12,13], or the generation of entangled states in a deterministic fashion of two [14] or more particles [15]. The maintenance of spin polarization in gases [16] and the dosage reduction in neutron tomography have also been studied [17].

Recently, an experiment using single photons within a micropillar cavity in a strong coupling limit was presented by Leppenen et al. [18]. Additionally, an experiment has been performed in which it is possible to predict if a quantum jump will occur, without invoking the QZ dynamics [19]. In such work, a two-level atom coupled to a third level is, again, employed. A detailed theoretical analysis of the latter reference is presented in [20].

In this work, we show that the control of population levels and the coherence can be performed with Zeno-type measurements, i.e., a succession of short "measurements pulses" during a π pulse in V-type systems.

We study how the population of the levels is modified as the sequence and/or the field strength of the measurement pulses is changed. In doing this, we describe the system based on its density matrix and then obtain the Bloch equations in a similar way to that described in reference [6].

Then, we return to the view of Cook and Itano, in which the three-level system is divided into a "quantum system" and a "measurement system", and we calculate the Von Neumman entropy of "the measurement system" with a single field mode used as auxiliary to perform the measurements.

We also comment, based on such simulations, on how "strong" the light–atom interaction must be in order to really alter the evolution of a system or, in Von Nuemann's interpretation, to produce a "collapse of the wavefunction". Finally, we present some examples of how, having a desired target of population distribution, such a goal can be obtained via an adequate pulse sequence.

2. The Model

Let us consider a system with a level structure in V, as shown in Figure 1. Levels $|b\rangle$ and $|c\rangle$ are linked through a constant decay γ. The spontaneous decay from level $|a\rangle$ to level $|b\rangle$ is long compared to γ, such that it is not taken into account for the purposes of the calculation. We also assume that the fields linking $|b\rangle \leftrightarrow |a\rangle$ and $|b\rangle \leftrightarrow |c\rangle$ are at resonance.

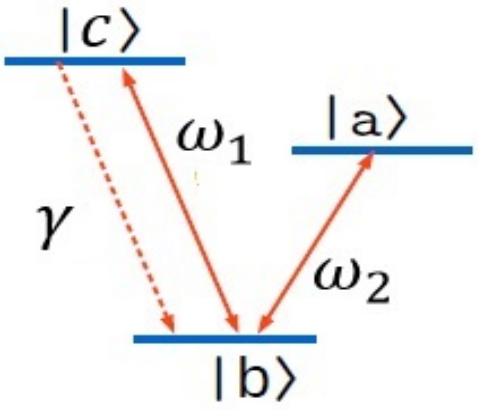

Figure 1. Three-level atom in V configuration, ω_1 is the frequency of an external field $\mathbb{E}_1$ and ω_2 is the frequency of an external field $\mathbb{E}_2$, interacting with the transitions $|b\rangle \leftrightarrow |c\rangle$ and $|b\rangle \leftrightarrow |a\rangle$, respectively.

In order to describe this system, we first present the Hamiltonian of the three-level atom coupled to two electromagnetic fields and then present the Bloch equations in the rotating wave approximation.

The Hamiltonian solely for the tree level atom can be written as

$$H_A \;=\; E_c|\,c\rangle\,\langle c| + E_a|\,a\rangle\,\langle a| + E_b|\,b\rangle\,\langle b| \tag{1}$$

The (classic) electromagnetic fields are given by:

$$\mathbb{E}_1(t) \;=\; \mathcal{E}_1(e^{-i\omega_1 t} + e^{i\omega_1 t}) \quad \text{and} \quad \mathbb{E}_2(t) \;=\; \mathcal{E}_2(e^{-i\omega_2 t} + e^{i\omega_2 t}) \tag{2}$$

where ω_1 and ω_2 are the frequencies of the fields $\mathbb{E}_1(t)$ and $\mathbb{E}_2(t)$, respectively. As usual, the Rabi frequencies are:

$$\Omega_1 \;=\; \frac{\mathcal{E}_1\mathcal{P}_{cb}}{\hbar} \quad \text{and} \quad \Omega_2 \;=\; \frac{\mathcal{E}_2\mathcal{P}_{ab}}{\hbar} \tag{3}$$

with $\mathcal{P}_{ij}$ as the dipole moment of the ij transition.

The full Hamiltonian of the system , i.e., the atom plus the interaction with the two fields, is given by

$$H_{Tot} = H_A + H_{int} \tag{4}$$

where

$$H_{int} = -\mathcal{P}_{cb}\mathbb{E}_1(t) - \mathcal{P}_{ab}\mathbb{E}_2(t) \tag{5}$$

In matrix form, H_{Tot} can be written as:

$$\begin{pmatrix} E_c & 0 & -\mathcal{E}_1\mathcal{P}_{cb}e^{-i\omega_1 t} \\ 0 & E_a & -\mathcal{E}_2\mathcal{P}_{ab}e^{-i\omega_2 t} \\ -\mathcal{E}_1\mathcal{P}_{cb}e^{i\omega_1 t} & -\mathcal{E}_2\mathcal{P}_{ab}e^{i\omega_2 t} & E_b \end{pmatrix} \tag{6}$$

where $\mathcal{P} = \mathcal{P}^*$.

Recalling that, in this model, there is spontaneous decay only from $|c\rangle \to |b\rangle$ (constant decay γ). With these elements, we can find the Bloch equations in the rotating wave approximation (RWA) [21]:

$$\begin{array}{rl} \dot{\rho}_{aa}(t) = & -\Omega_2 v_{ab} \\ \dot{\rho}_{bb}(t) = & -\Omega_1 v_{cb} + \gamma\rho_{cc} + \Omega_2 v_{ab} \\ \dot{\rho}_{cc}(t) = & -\Omega_1 v_{cb} - \gamma\rho_{cc} \\ \dot{u}_{ca}(t) = & \Omega_2 v_{cb} + \Omega_1 v_{ab} - \frac{\gamma}{2}u_{ca} \\ \dot{v}_{cb}(t) = & 2\Omega_1 w_{cb} + \Omega_2 u_{ca} - \frac{\gamma}{2}v_{cb} \\ \dot{v}_{ab}(t) = & 2\Omega_2 w_{ab} + \Omega_1 u_{ca} \\ \dot{w}_{cb}(t) = & -2\Omega_1 v_{cb} - \Omega_2 v_{ab} - 2\gamma\rho_{cc} \\ \dot{w}_{ab}(t) = & \Omega_2 v_{av} - \Omega_1 v_{cb} - \gamma\rho_{cc} \end{array} \tag{7}$$

where, as is usual in this kind of representation, ρ_{ii} is the probability of finding the population in the i level, u_{ij}, v_{ij} and w_{ij} are the components of the Bloch vector for this three-level system, Ω_1 is the Rabi frequency between levels $|b\rangle \leftrightarrow |c\rangle$ and Ω_2 is the Rabi frequency between $|b\rangle \leftrightarrow |a\rangle$. We also mention that the terms involving the long $|a\rangle \to |b\rangle$ decay time have already been discarded. Note that the last two equations above are not independent of the previous ones, so, when this system, it is only necessary to take into account the first six equations.

As Itano et al. discussed in their paper, the transition $|b\rangle \leftrightarrow |a\rangle$ is taken as the quantum system being monitored and the transition $|b\rangle \leftrightarrow |c\rangle$ together with pulses at the field mode at ω_1 as the measurement system which, at each pulse, projects the wave function either into $|b\rangle$ or $|a\rangle$. This experiment has been taken as the prototype for the confirmation of freezing of the evolution of an induced transition.

On the other hand, Frerich et al. described this experiment as the evolution of a "V"-type three-level system coupled to two field modes, each of them connecting the ground state with one of the upper states (Figure 1), with the Hamiltonian governing its evolution as in Equation (4). For these systems, it is not necessary to invoke the projection postulated, but to realize that is the dynamics described by the set of equations in (7).

We also can use the set of equations in (7) to vary the different parameters involved there. In particular, we will focus our attention on the number of measurement pulses and/or their strength, i.e, the value of Ω_1, and look at the changes that these parameters introduce to the system's behaviour, from pure Zeno dynamics to a route that allows us to control the population in each state.

In Sections 3.1 and 3.2, we will look at the effects of the dynamics by changing the mentioned parameters and how, when the Ω_1 strength goes beyond saturation, the freezing of the system's evolution is recovered.

Later (Section 3.3), by once again taking the view of a quantum system and a measurement system, we perform the calculation of the time evolution of the entropy for the latter (the measurement system) with the field with frequency ω_1.

In the Itano experiment, the authors performed the experiment with Be ions confined in a Penning trap. The bandwidth of the transition they used was $\gamma = 2\pi \times 19.4$ MHz [22]. In order to be able to make quick comparisons with those results, Frierich at al. fitted their simulations to the parameters of such experiment. According to the same idea, we have implemented something similar with the parameters in our simulations.

Firstly, with Equation (7), we want to reproduce the freezing of the system's evolution (the Zeno effect) so, we take at $t = 0$ all the population being in the ground state $|b\rangle$ and take the case when $\Omega_2 << \Omega_1$.

We consider a π-pulse ($\pi = 2\Omega_2 t$) between levels $|b\rangle$ and $|a\rangle$. As "measuring pulses", n pulses are applied over the duration of the π-pulse at time intervals of γt_1 with pulse width of γt_2 (as can be seen in Figure 2b) and frequency $\Omega_1 = \gamma$. We point out that, in the units we are using here, a full π pulse corresponds to $\gamma t \approx 2405$ and the saturation of the transition $|b\rangle \rightarrow |c\rangle$ corresponds to $\Omega_1 \approx 900$.

We point out that these results coincide, as expected, with those of Frerichs et al. (see Figure 4 in reference [6]).

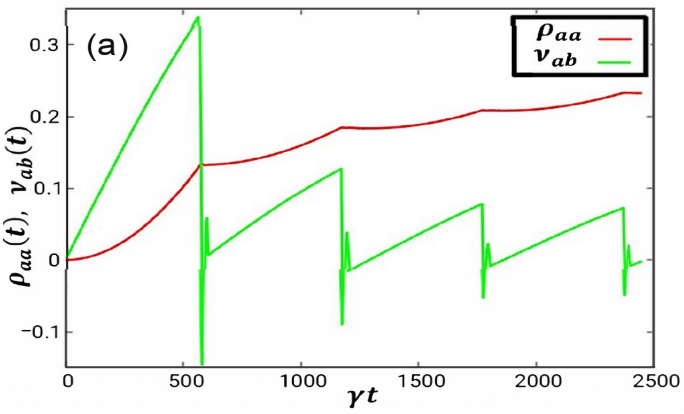

Figure 2. *Cont.*

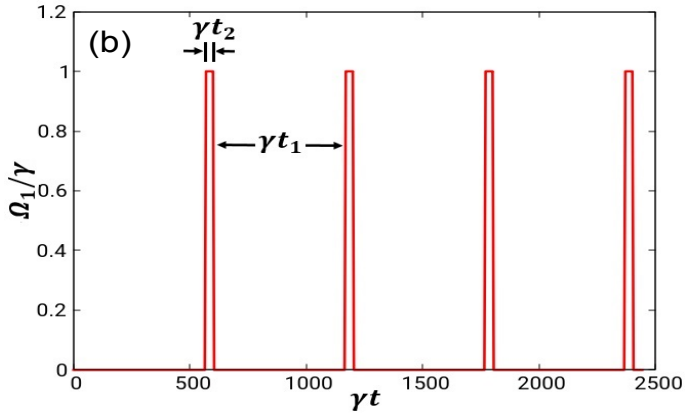

Figure 2. (**a**): Time evolution of the population in the $|a\rangle$ state and the coherence V_{ab}, the values for this simulation are $\Omega_1 = 900$, $\Omega_2 = 3.2656$, $\gamma t_1 = 566$ and $\gamma t_2 = 35$. (**b**): sequence of "measuring pulses" with $n = 4$.

3. Results

In this section, we present numerical results when some of the parameters that can be controlled in a Zeno-type experiment are varied in order to observe their influence on the evolution of the V system under consideration.

3.1. Weak "Measurement Pulse" and Few Pulse Measurements

In this set of results, we analyse when the strength of the interaction is "weak" either because (a) the amplitude of the measuring field is itself low, i.e., $\Omega_1 \geq \Omega_2$ or (b) because the number of measurements is small or (c) both of these instances at the same time.

For each of these cases, the system is prepared with 100% of its population occupying level $|b\rangle$.

Figure 3 shows the population evolution of each level when $\Omega_1 = \Omega_2$ for 12 measurements pulses (Figure 3a) and for 52 measurements pulses (Figure 3b). We can see that, with the same value for the Rabi frequency, with few measurement pulses, almost no population is transferred to level $|c\rangle$, as we can expect because of the weak interaction. However, as the number of measurement pulses is increased, the share of population of level $|c\rangle$ is slightly increased, even if we have this weak interaction.

This evolution is also shown when $\Omega_1 = 20$ and $\Omega_2 = 3.256$ for $n = 12$ (Figure 3c) and $n = 52$ (Figure 3d), respectively. Again, we can see that changing the number of measurement pulses alters the evolution of the atomic population. In this particular instance, as Ω_1 is about six times the value of Ω_2 and $n = 12$ the population share between levels $|c\rangle$ and $|a\rangle$ is practically the same (Figure 3c). On the other hand, when n is increased to 52 (Figure 3d), the population in level $|c\rangle$ is greatly increased.

So, when we have $\Omega_1 \approx \Omega_2$ or Ω_1 a few times bigger than Ω_2, by changing the number of measurement pulses (and, consequently, the time interval between measurements γt_1) the behaviour of the population transfer can be deeply altered.

Now, in Figure 4, we have eight measurement pulses in the full π pulse but this time $\Omega_1 = 700$. In this case, the population of the system is mostly (and equally) distributed between $|b\rangle$ and $|c\rangle$ with a smaller fraction of the population for level $|a\rangle$, as can be expected because the stronger interaction between levels $|b\rangle$ and $|c\rangle$ is dictated by the value of Ω_1.

Note that, in the examples of Figures 3d and 4, the maximum transfer of population to level $|a\rangle$ is similar (about 10%); however, the change in the number of measurement pulses and the increased value of Ω_1 lead to a very different share of the population between levels $|b\rangle$ and $|c\rangle$. So, not just the value of the Rabi frequency Ω_1 may alter the population transfer but also, in combination with a change in n, the population sharing among the three available levels can be altered.

Figure 5 shows two examples of how ρ_{aa} changes when the strength of the external field is low (below saturation) and the number of measurement pulses is increased from

0 up to 52, $\Omega_1 = 20$ for Figure 5a and $\Omega_2 = 100$ for Figure 5b. In this case, the Zeno Effect may not occur, regardless of the number of measurements made. We can see that for each measurement n, the trajectory of the population density ρ_{aa} cannot be kept constant over time as is expected in a Zeno dynamic. Recall that, as n increases, there is different temporal spacing for γt_1, as defined by Figure 2.

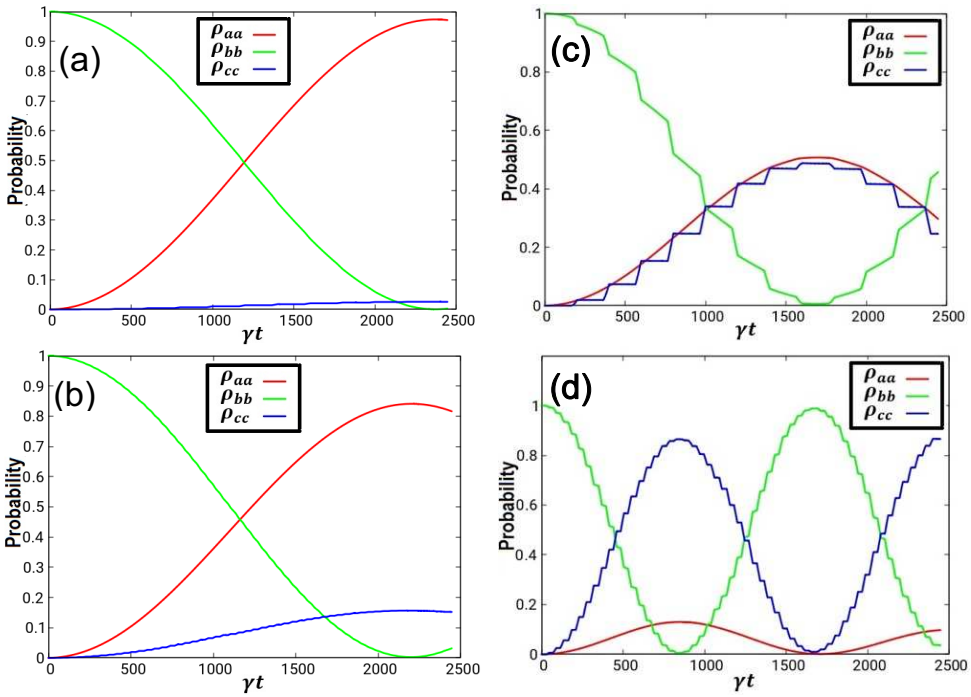

Figure 3. Atomic population evolution with (**a**) $n = 12$, $\Omega_1 = \Omega_2 = 3.256$, (**b**) $n = 52$, $\Omega_1 = \Omega_2 = 3.256$ (**c**) $n = 12$, $\Omega_1 = 20$, $\Omega_2 = 3.256$, (**d**) $n = 52$, $\Omega_1 = 20$, $\Omega_2 = 3.256$. When $n = 12$ measurement pulses, then $\gamma t_1 = 165.5$, $\gamma t_2 = 35$. When $n = 52$, $\gamma t_1 = 26.25$, $\gamma t_2 = 20$. For all graphs $\gamma = 0.1$,

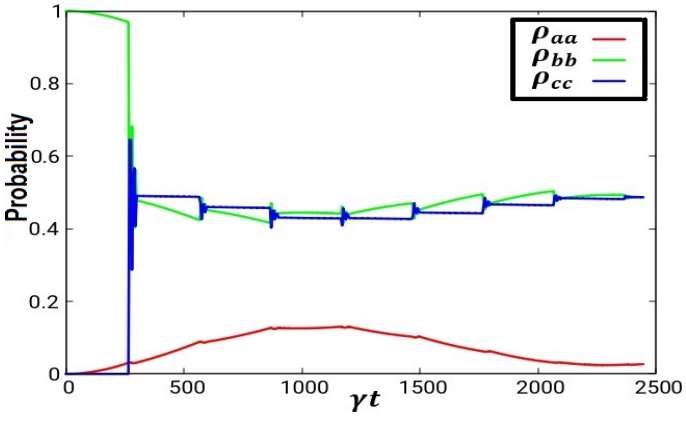

Figure 4. Population evolution with $\gamma = 0.1$, $\Omega_1 = 700$, $\Omega_2 = 3.2656$ for the case of few measurements and strong interactions ($n = 8$, $\gamma t_1 = 265.6$, $\gamma t_2 = 35$).

In the 3D graphics below, when there are no measurement pulses, ($n = 0$) is just the coherent transfer of population form level $|b\rangle$ to $|a\rangle$; then, as the number of measurements pulses increases, we can see how the evolution of the system changes, although it is not enough to freeze the system's evolution. It is worth to note that, from an ideal Zeno experiment, the number of measurement pulses grows towards infinity; then, even if the external field Ω_1 is "low", the continuous measurement will freeze the evolution of our system. However, in a real experiment, both γt_1 and γt_2 are finite and there is a maximum

of these time intervals that can be accommodated in a π pulse, so in practice we are limited in how many pulses we can apply and whether or not the Zeno-behaviour can be achieved.

In Figure 5, as we can see, stronger interaction with the external field results in a more complex evolution with more oscillations, although they are smaller in amplitude. For the first example (Figure 5a), we go from the coherent transfer of population to, as n grows, just a couple of oscillations in ρ_{aa}. When Ω_1 is increased (Figure 5b), we can notice that, with n up to around 20, we predominantly observe a population transfer to level $|a\rangle$. However, while increasing the number of measurement pulses, we enter a behaviour with more oscillations but a smaller amplitude, i.e., towards a freezing of the population in level $|a\rangle$. So, as stated before, in the limit where the duration of the measurement pulses decreases and the number of measurement pulses is increased, we would recover the Zeno dynamics.

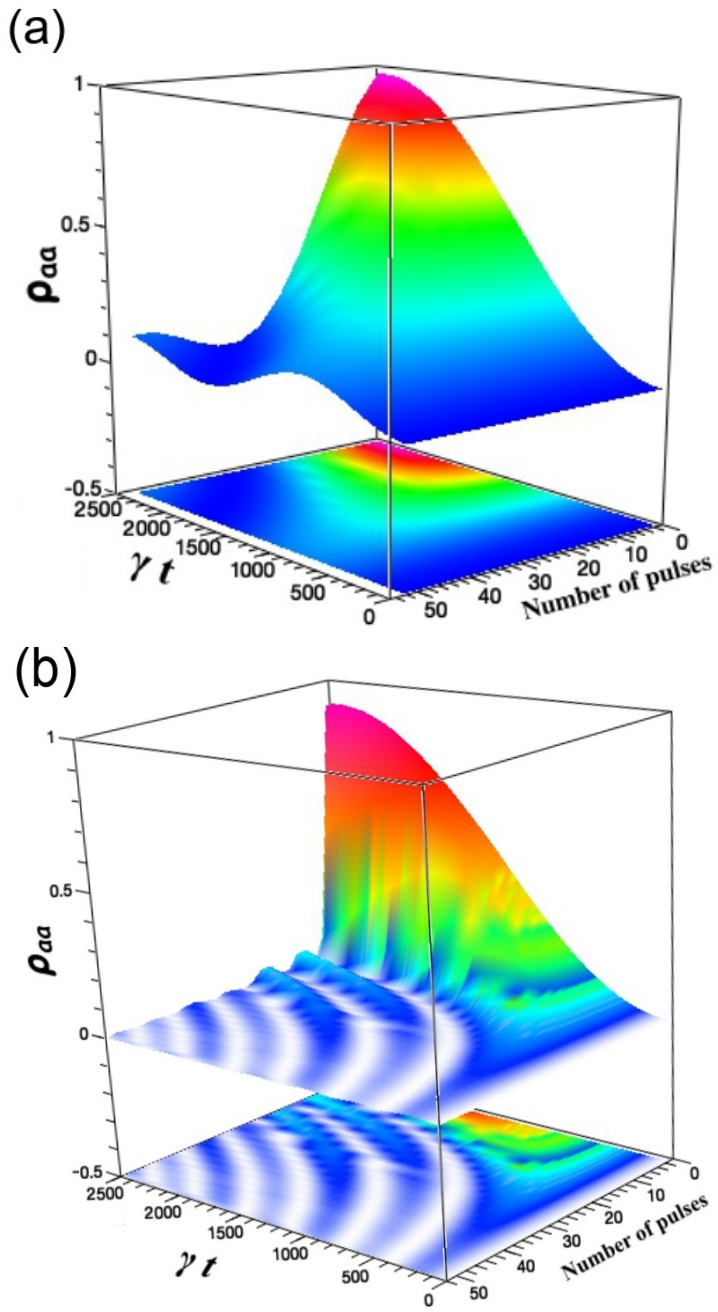

Figure 5. Population evolution ρ_{aa} as the number of measurements pulses changes from $n = 0$ up to $n = 52$. (**a**) with $\Omega_1 = 20$, $\gamma = 0.1$, $\Omega_2 = 3.2656$. (**b**) with $\Omega_1 = 100$, $\gamma = 0.1$, $\Omega_2 = 3.2656$. Colors are added to appreciate better the oscillations in the graph, no specific physical meaning is intended.

So far, in the examples shown above, we have seen that the behaviour of the population transfer within a π pulse can be greatly modified either by changing the number of measurement pulses or by changing the strength of the interaction between levels $|b\rangle$ and $|c\rangle$.

So, what would happen if we keep increasing the value of Ω_1 until saturation?

3.2. Freezing of Atomic Populations by Measurement Pulses beyond Saturation

The graphs we present below show the manipulation of the trajectories of the three atomic levels. They have in common that during the π pulse and decay γ, the levels $|c\rangle$ and $|b\rangle$ interact strongly through Ω_1, i.e, at the saturation intensity (or above) of the $|b\rangle$ to $|c\rangle$ transition, with $n = 52$ and consequently short time intervals γt_2.

In Figure 6 we present a case in which the population has been equally prepared, such that $\rho_{aa} = \rho_{bb} = \rho_{cc} = 33\%$. Under this strong interaction and at the scale of the figure, there seems to be no variation in the ρ_{ii} (i = a,b,c) levels and each population level remains constant (Figures 6 and 7).

However, zooming in on Figure 6, we can observe that indeed there is a very small population oscillation between states $|b\rangle|$ and $|c\rangle$ dictated by the applied pulses at Ω_1. So, in a coarse scale, we can not see a change in the population levels. Just when we go to a finer scale (the third decimal figure) the small population exchanges can be observed. Note, that for this graph, the three lines (red, green and blue) are also superimposed.

So, under strong Ω_1 interaction, as we see in Figure 6, the $|b\rangle|$, $|c\rangle$ and $|a\rangle$ states maintain the initial population distribution, no matter how the system is originally prepared.

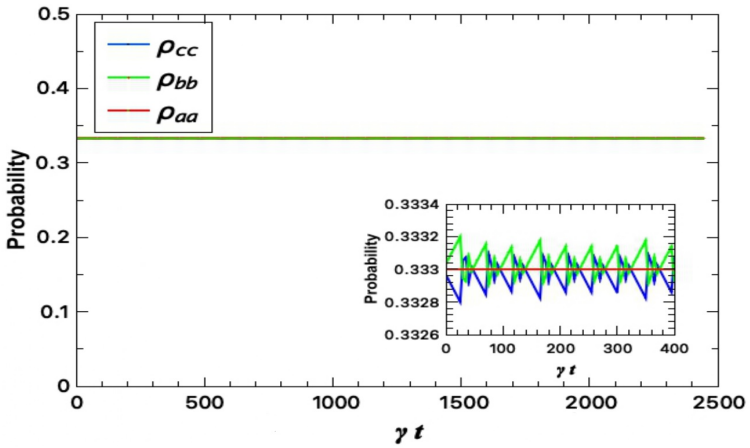

Figure 6. Population distribution during the π-pulse. $\Omega_1 = 1000$, $\gamma = 0.1$, $\Omega_2 = 3.2656$, $\gamma t_2 = 20$, $\gamma t_1 = 26.25$. Initial conditions: $\rho_{aa} = \rho_{bb} = \rho_{cc} = 33\%$.

Similarly, Figure 7 shows, as in the previous figure, over the duration of the π pulse, there is no change in population under the condition of a strong interaction mediated by a large Ω_1.

Of course, the examples shown above are classical archetypes of Zeno dynamics. Here, they are shown in order to compare what happens when there is very strong interaction by setting Ω_1 well above saturation, opposite to what we saw in the previous section when we modified either n or the value of Ω_1.

3.3. Entropy and the Role of Ω_1 Strength

Let us determine the entropy between the measuring system with a single mode field $\mathbb{E}_1$ with frequency ω_1. As we will see in what follows, the entropy is at its maximum when we have a Zeno-type dynamic, no matter what the initial population distribution might be.

As this system is bipartite, the Schmidt decomposition guarantees that for any instant in time t, we find bases $\{|U_1(t)\rangle\}$ for the atom and $\{|V_1(t)\rangle\}$ for the field, such that state of the system can be written as

$$|\Psi(t)\rangle \ = \ \lambda_1(t)|U_1(t)\rangle|V_1(t)\rangle + \lambda_2(t)|U_2(t)\rangle|V_2(t)\rangle \tag{8}$$

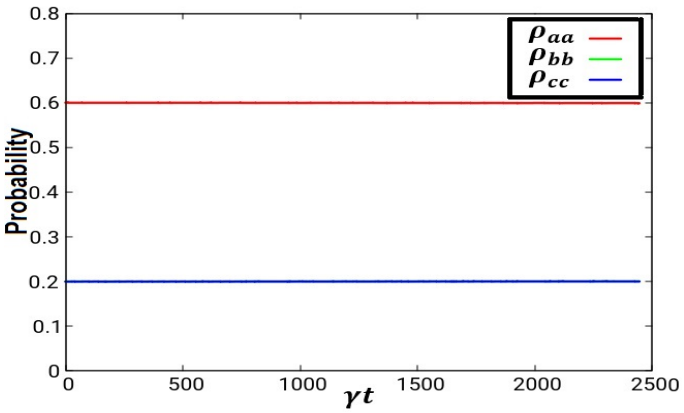

Figure 7. Population distribution during π-pulse $\Omega_1 = 1000$, $\gamma = 0.1$, $\Omega_2 = 3.2656$, $\gamma t_2 = 20$, $\gamma t_1 = 26.25$. Initial conditions: $\rho_{aa} = 60\%$, $\rho_{bb} = \rho_{cc} = 20\%$. As $\rho_{bb} = \rho_{cc}$ the green curve in the figure is hidden by the blue curve.

We also find that the reduced density matrices of the atom and field in these bases are identical

$$\rho_U(t) \ = \ \rho_V(t) = \begin{pmatrix} |\lambda_1(t)|^2 & 0 \\ 0 & |\lambda_2(t)|^2 \end{pmatrix} \tag{9}$$

Based on Equation (7), we parameterize the density matrix in this basis specified by $|b\rangle$ and $|c\rangle$ with components of the Bloch vector [23]

$$u_{cb}(t) = \rho_{cb}(t) + \rho_{bc}(t) \tag{10}$$

$$v_{cb}(t) = i[\rho_{cb}(t) - \rho_{bc}(t)] \tag{11}$$

$$w_{cb}(t) = \rho_{cc}(t) + \rho_{bb}(t) \tag{12}$$

and then we obtain

$$\lambda_{1,2} = \frac{1}{2}\left[1 \pm \sqrt{u_{cb}^2 + v_{cb}^2 + w_{cb}^2}\right] \tag{13}$$

where we know that, for a mixed state $\sqrt{u_{cb}^2 + v_{cb}^2 + w_{cb}^2} < 1$ holds.

Then, to numerically evaluate the entropy between the measurement system and a single electromagnetic field mode (ω_1), we use the Von Neumann entropy [24]:

$$S(t) \ = \ |-\lambda_1(t)|^2 log_2|\lambda_1(t)|^2 - |\lambda_2(t)|^2 log_2|\lambda_2(t)|^2 \tag{14}$$

Figure 8 shows the time evolution of entropy for different frequency values of Ω_1 and different sets of initial population values. For these simulations, the parameters γt_2, γt_2, γ, Ω_2 and n are as described in Figures 6 and 7.

In the first three instances, the initial population has been set in just one of the three levels of the system. In the next three examples, a mixture of populations among the levels was prepared.

The first obvious observation is that, as the value of Ω_1 is increased towards saturation and beyond, we obtain a Zeno-type dynamic—where the population distribution is

frozen—and the entropy rapidly tends to its maximum and remains there for the whole simulation.

Is also worth pointing out that, as general trends from these graphics, if the system is prepared with all its population either in $|b\rangle$ or $|c\rangle$, regardless of the Ω_1 value, the entropy starts with a value of zero, whereas if the system in prepared in $|a\rangle$, the entropy always will start at its maximum possible value.

In Figure 8d, where the simulation is prepared with $\rho_{aa} = \rho_{cc} = 0.5$ and no population in level $|b\rangle$, we can observe that the entropy does not begin at its maximum value, like in Figure 8a, nor in zero, as in Figure 8b or Figure 8c. Meanwhile, for Figure 8e,f, where at the beginning there is population en each of the three levels (although with different proportions) and specially as level $|a\rangle$ is populated, the entropy starts from the maximum value. Note that, for these last two examples, there are variations in the entropy, but the size of them is very small, and its value always lays very close to the maximum.

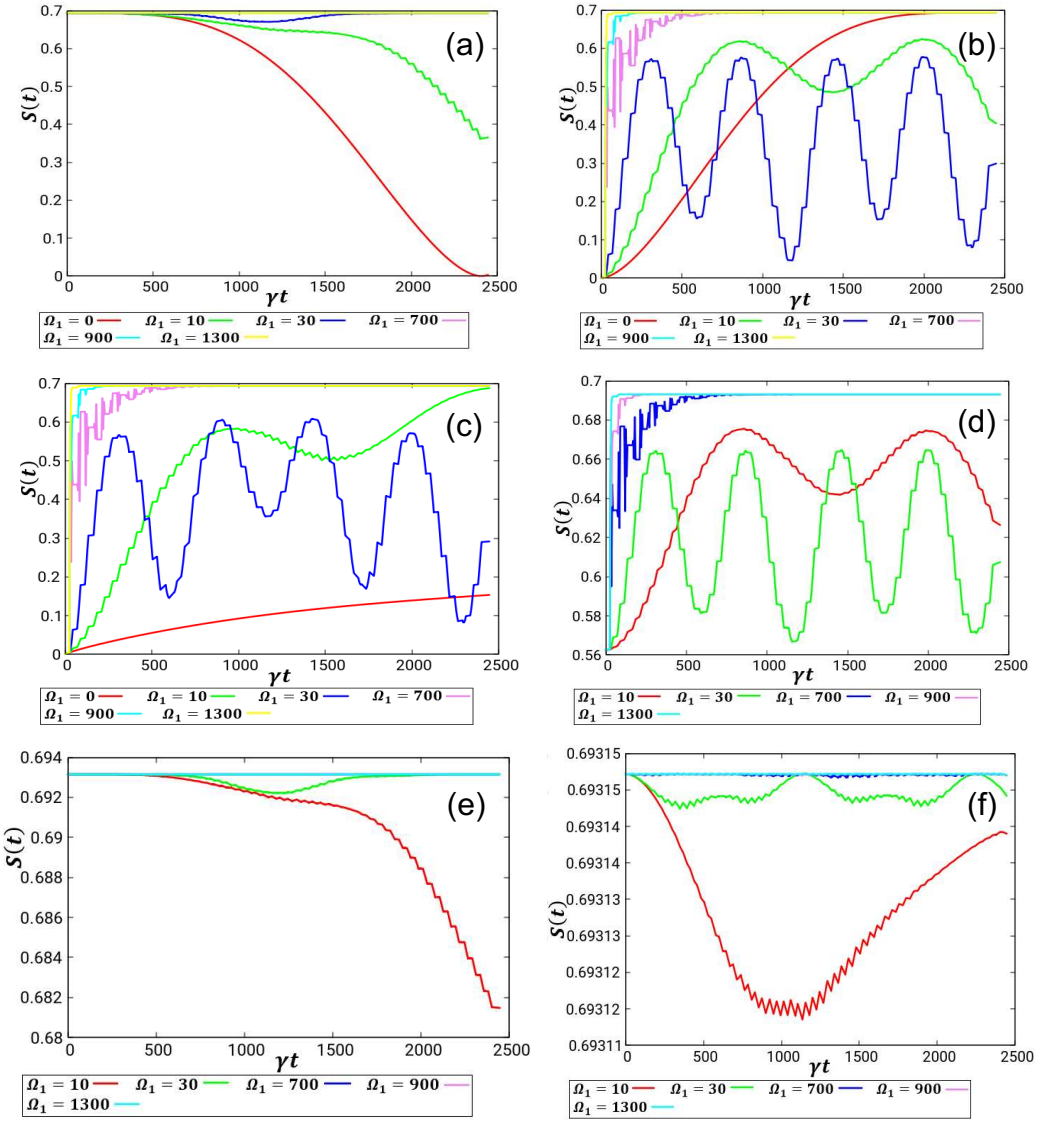

Figure 8. Entropy evolution, for all the graphics shown here, γt_2, γt_2, γ, Ω_2 are as described in Figure 7 and $n = 52$. For each curve, the Ω_1 strength was changed as indicated. Initial population distributions: (**a**): $\rho_{aa} = 1$, $\rho_{bb} = 0$, $\rho_{cc} = 0$. (**b**): $\rho_{aa} = 0$, $\rho_{bb} = 1$, $\rho_{cc} = 0$, (**c**): $\rho_{aa} = 0$, $\rho_{bb} = 0$, $\rho_{cc} = 1$. (**d**): $\rho_{aa} = 0.5$, $\rho_{bb} = 0$, $\rho_{cc} = 0.5$. (**e**) $\rho_{aa} = 0.2$, $\rho_{bb} = 0.4$, $\rho_{cc} = 0.4$. (**f**): $\rho_{aa} = \rho_{bb} = \rho_{cc} = 1/3$.

So, we also could interpret changes in entropy as a measure of what the strength of Ω_1 should be in order to alter the evolution of these kinds of systems, from a pure coherent evolution ($\Omega_1 = 0$) to a Zeno-type dynamic when $\Omega_1 > 100$ and well beyond saturation, in which we have freezing of the atomic populations.

3.4. Driving a System via Zeno-Type Measurements

Here, we present the driving of an atomic V-type three level system via Zeno-type measurements combined with periods of free evolution while also showing the calculation of entropy between the levels $|b\rangle$ and $|c\rangle$.

Figure 9a presents a system evolving from its initial state (with all the population in $|b\rangle$) where the pulse driving the $|b\rangle \leftrightarrow |a\rangle$ transition has been applied until $\gamma t = 1920$. By then, 90% of the population has been transferred to state $|a\rangle$ and the rest has been distributed to the other two states, i.e., it is just a typical example of coherent transfer of population where the driving pulse has been paused before finishing the full π pulse. Figure 9b shows the entropy of the event.

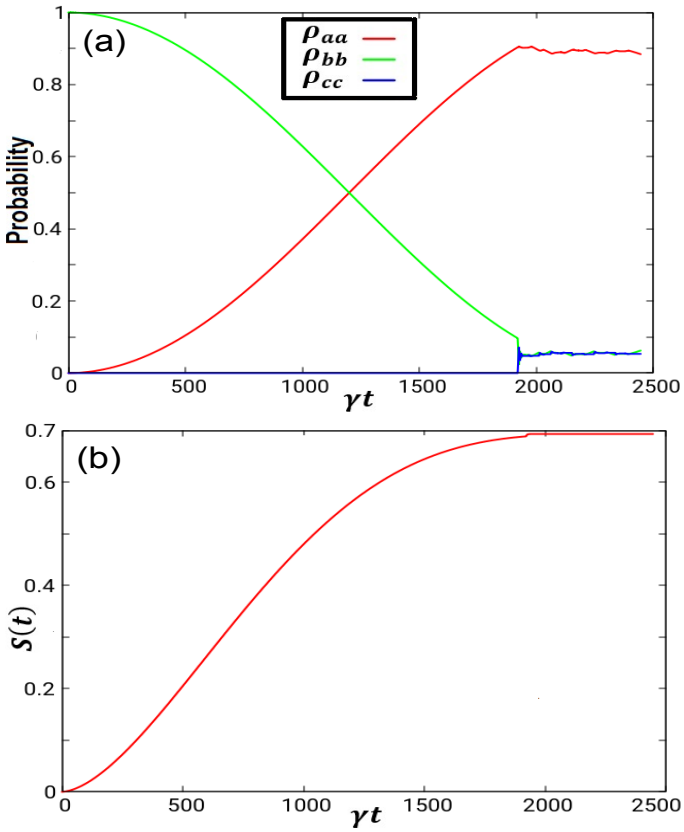

Figure 9. Population distribution during π-pulse. Initial conditions (**a**): $\rho_{aa} = 0.0\%$ $\rho_{bb} = 100\%$, $\rho_{cc} = 0.0\%$, $\Omega_1 = 1000$, $\gamma = 0.1$, $\Omega_2 = 3.256$, $\gamma t_2 = 20$, $\gamma t_1 = 26.25$. (**b**): entropy evolution.

In Figure 10a, we present an example where, from the start of the simulation and up to $\gamma t = 2405$, all the population is equally split in states $|b\rangle$ and $|c\rangle$ and no population in $|a\rangle$, while a π-pulse and measurement pulses ($n = 52$) with $\Omega_1 = 1000$ are applied.

This time, we follow the evolution of the system for a time equivalent to $\gamma t = 40{,}000$. After the time $\gamma t = 2405$ (the duration of the π-pulse) just the Ω_2 is left on and no more measurement pulses are applied. As can be observed in the figure, we have a coherent evolution between states $|a\rangle$ and $|b\rangle$ and the decaying of the population of level $|c\rangle$, in this case from 0.5 to around 0.22 in the simulation time showed here. As level $|c\rangle$ decays, the population lost by this level is gained by the other two. Figure 10b shows the entropy evolution of this example.

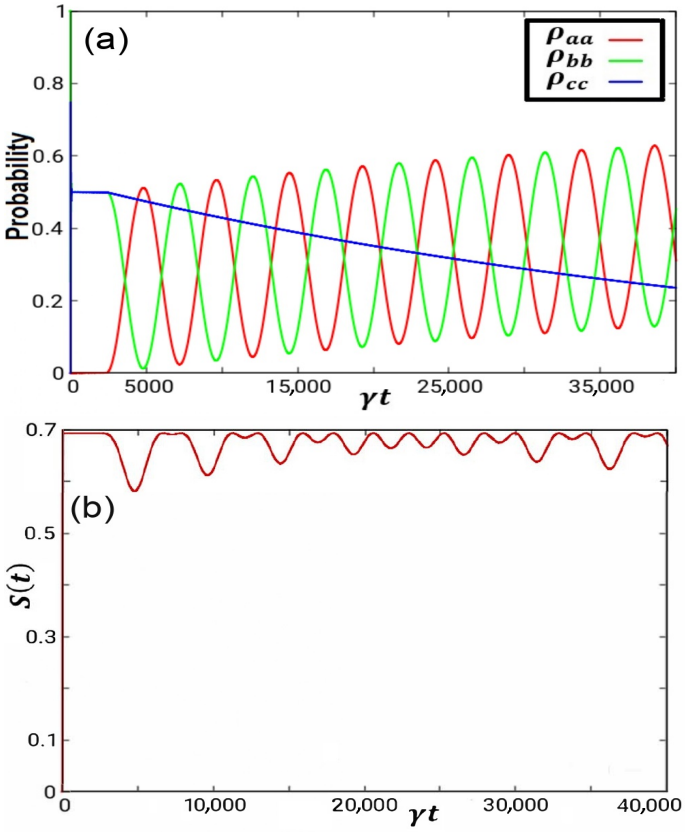

Figure 10. Driving atomic levels. Initial conditions (**a**): $\rho_{aa} = 0.0\%$, $\rho_{bb} = \rho_{cc} = 50\%$ $\Omega_1 = 1000$, $\gamma = 0.1$, $\Omega_2 = 3.2656$, $\gamma t_2 = 20$, $\gamma t_1 = 26.25$. (**b**): entropy evolution

Figure 11 shows an example where, starting from a population distribution of 33% in each level, we have just the presence of the Ω_2 with no measurement pulses from the very beginning; hence, we obtain the coherent evolution of the levels $|a\rangle$ and $|b\rangle$ and the decay from level $|c\rangle$.

So, assume that for a particular experiment and starting from the initial conditions illustrated in Figure 11, we would need to reach a population of 25% in level $|c\rangle$. We could wait a period equivalent to $\gamma t = 15{,}000$ and from there start with measurement pulses with Ω_1 larger than the saturation intensity, so the population in $|c\rangle$ (and $|b\rangle$ and $|a\rangle$) will remain constant.

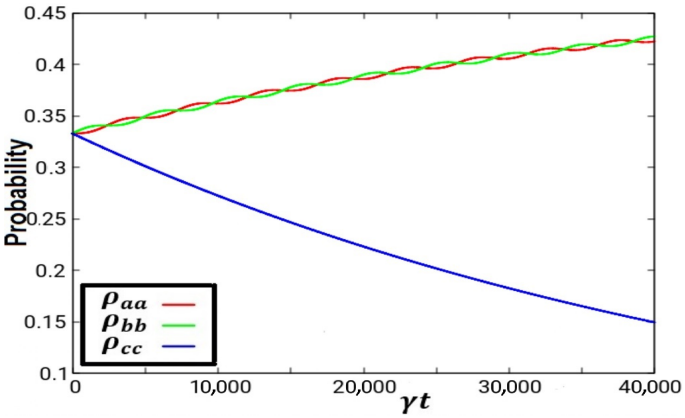

Figure 11. Initial conditions $\rho_{aa} = \rho_{bb} = \rho_{cc} = 33$ %, $\Omega_1 = 0.0$, $\gamma = 0.1$, $\Omega_2 = 3.2656$

So, we can have a method that starts from some arbitrary set of initial values for the population levels, allowing us to design a sequence of Zeno-type measurements (i.e., a

π-pulse and measurements pulses) followed by time intervals when Ω_1 or Ω_2 (or both) are present to reach a desired final population distribution set.

As an example, in Figure 12, once again we start with a population distribution of 33% in each level. From there, a Zeno-type interval which keeps the populations unchanged, followed by a period where just the Ω_2 field is present (with the concomitant decay from level $|c\rangle$), then another time interval (from γt = 7615 up to γt = 10,000) when Zeno-type measurement is applied, so the population distribution remains unchanged. Note that the population in $|a\rangle$ has been increased to 35%. From there, and up to γt = 23,200, neither Ω_1 nor Ω_2 are present, so, the population from level $|c\rangle$ starts to decay to $|b\rangle$ and the population in $|a\rangle$ remains constant as, in this time scale, decay from $|a\rangle$ to $|b\rangle$ plays no role. From γt = 23,200 up to 25,500, just Ω_2 is present, so we have coherent evolution of $|a\rangle$ and $|b\rangle$ while $|c\rangle$ continues its decay. Finally, from 25,500 up to 30,000, a new period of Zeno-type dynamics is applied, such that population in $|a\rangle$ reaches 40% while the rest of the population is equally distributed between $|b\rangle$ and $|c\rangle$. Figure 12b shows the entropy evolution of this example.

So, we have shown a simple example of how the population distribution can be manipulated to obtain a different share of the population among the accessible states by applying different pulse sequences.

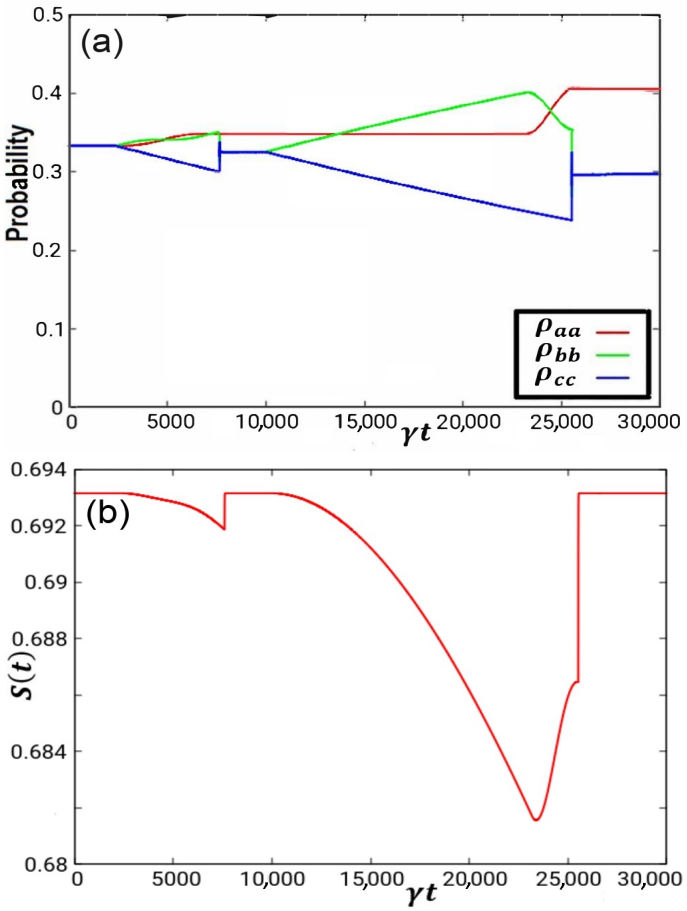

Figure 12. Driving atomic levels. (**a**): Drive the system to able to ρ_{aa} = 40%, $\rho_{bb} = \rho_{cc}$ = 30% Ω_1 = 1000, γ = 0.1, Ω_2 = 3.2656, γt_2 = 20, γt_1 = 26.25. (**b**): entropy evolution.

3.5. Discussion

In this paper, we have shown numerical calculations based on the description, with Bloch equations, of a V-type atomic system, and presented its evolution when subject to two electromagnetic fields, one inducing a π-pulse and a second one being used as a sequence of "measurement pulses" within the time interval of the π-pulse. This represen-

tation has been used before to describe Zeno-type dynamics. Here, we use it in a more general fashion, as we explore what occurs when some of the parameters relevant to the model are changed such that an incomplete Zeno dynamic is obtained.

In Section 3.1 we analyze some of the consequences of varying either the number (n) of applied measurements pulses or the strength (Ω_1). We have seen that when the number of measurements pulses is reduced and/or the Ω_1 is changed, the evolution of the population at each level may be profoundly altered, which in turn, suggests a method that could be used to control the time-evolution of the atomic populations in each level. In Section 3.2, we have shown typical examples of Zeno-type dynamics when the strength of Ω_1 is well above saturation, in comparison with the previous section. We recall that Zheng et al. [25] have shown experimentally in NMR qubits that by changing the measurement pulse duration (γt_2 according to our notation) the Zeno dynamics can be changed or even be suppressed. So indeed, Zeno-type dynamics can be used to control the evolution of a qubit.

Section 3.3 shows the results where Ω_1 is changed, from well above saturation towards $\Omega_1 \rightarrow$ zero. As we have seen, from saturation and beyond, we already know we have Zeno-type dynamics and in the graphics of this section, we can observe that the value of the entropy always reaches the maximum. So, although the entropy is calculated between the "auxiliary" measurement system and the single mode field (ω_1), if this quantity is maximized and remains constant during the simulation, then we know that we have a Zeno-type dynamic where the population in all three levels remains constant.

It is also interesting to ask a general question about the minimum field strength (or "how many photons are needed") required to change the dynamics of a system, and this study may pave the way to a more systematic study of such a question. Based on earlier experiments with atoms with few photons in cavities, it can be argued that just one is enough; in this cavity-assisted system, we have quantum revivals with a mean photon number of one. However, in the situation studied here, we do not have the presence of the enhancing cavity but a three-level system (or an ensemble of them) confined in a region of space (by an ion trap, for example). In such a situation, we must still consider the valid question of whether one photon is enough to modify the dynamics of a system. We could phrase this question differently: how many photons are needed to collapse the wavefunction?

We have discussed how, starting from sequences of Zeno-type measurements and time intervals where just the Ω_2 field is applied, a control in the population distribution can be obtained for the system studied here. These results should be applicable to any type of V-type system, trapped atoms or solid state quantum qubits, for example. In Section 2, our simulations show that a careful combination of the strength of the measurements pulses and/or the number of them can greatly alter the evolution of the system.

Finally, in Section 3.4, we have shown that is possible to drive the population levels of a V-type system (within the limits of the Bloch equations), in principle, in a deterministic way, such that, starting with a given set of initial population in each level, we could reach any other desired distribution of population in each of the atomic levels as long as we can find a suitable sequence of pulse measurement combined with free evolution of the atom.

At this point, needless to say, in our simulations we have not intended to obtain the most efficient pulse sequence to achieve the fastest route from state A (initial populations $\rho_{ii}^{initial}$) to state B (ρ_{ii}^{final}). Such questions will be addressed in future studies.

3.6. Conclusions

As was mentioned before, for the implementation of quantum technologies, the best possible control of the diverse parts of the system must be achieved. In this context, we have presented results showing how, by changing the parameters normally used to induce a Zeno-type dynamics (the freezing of the atomic populations due to frequent measurements) in a V type system, control of the population levels can be achieved.

As intuition would suggest, we would expect that by changing the strength of the Ω_1 field, we can modify the system behaviour, as shown by the simulations. However, as we

have also presented, weak Ω_1 pulses combined with a change of the number of pulses can lead to a very different dynamical behaviour. We also showed how the calculation of the entropy is a useful parameter for determining whether we have a Zeno dynamics.

So, with a careful selection of relevant parameters such as the field strength or the number of the measurement pulses, the control of the population's levels can be realised. We have shown that for different initial conditions in the population levels, an appropriate sequence of pulses followed by time intervals when just one external field is present can be used to achieve any another needed distribution between the accessible states.

Author Contributions: All authors contributed equally to this research. All authors have read and agreed to the published version of the manuscript.

Funding: This research received no external funding.

Institutional Review Board Statement: Not applicable.

Informed Consent Statement: Not applicable.

Data Availability Statement: The data used to produce all the graphics shown in this article are available upon request to any of the authors.

Acknowledgments: JCS thanks the Mexican Consejo Nacional de Ciencia y Tecnología (CONACYT) for awarding a PhD scholarship. The authors are also grateful for the support provided by SNI-CONACYT, COFFA-IPN and EDD-IPN. The useful comments on the manuscript by E. Haro Poniatowski, C. A. Guarín Duran and L. G. Mendoza Luna are also very much appreciated.

Conflicts of Interest: The authors declare no conflict of interest.

References

1. Misra, B.; Sudarshan, E.C.G. The Zeno's paradox in quantum theory. *J. Math. Phys.* **1977**, *18*, 756–763. [CrossRef]
2. Cook, R.J. What are quantum jumps? *Phys. Scr.* **1988**, *T21*, 49–51. [CrossRef]
3. Itano, W.M.; Heinzen, D.J.; Bollinger, J.J.; Wineland, D.J. Quantum Zeno effect. *Phys. Rev. A* **1990**, *41*, 2295–2300. [CrossRef] [PubMed]
4. Khalfin, L.A. Contribution to the decay theory of a quasi-stationary state. *Sov. Phys. JETP* **1958**, *33*, 1371–1382.
5. Pokorny, F.; Zhang, C.; Higgins, G.; Cabello, A.; Klienmann, M.; Hennrich, M. Tracking the dynamics of an ideal Quantum Measurement. *Phys. Rev. Lett.* **2020** , *124*, 080401. [CrossRef] [PubMed]
6. Frerichs, V.; Schenzle, A. Quantum Zeno effect without collapse of the wavepacket. *Phys. Rev. A* **1991**, *44*, 1962–1968. [CrossRef] [PubMed]
7. Nakazato, H.; Namiki, M.; Pascazio, S.; Rauch, H. Understanding the quantum Zeno effect. *Phys. Lett. A* **1996**, *44*, 203–208. [CrossRef]
8. Facchi, P.; Nakazato, H.; Pascazio, S. From the quantum Zeno to the inverse quantum Zeno effect. *Phys. Rev. Lett.* **2001**, *86*, 2699–2703. [CrossRef]
9. Harrington, P.M.; Monroe, J.T.; Murch, K.W. Quantum Zeno effects from measurement controlled qubit-bath interactions. *Phys. Rev. Lett.* **2017**, *118*, 240401. [CrossRef]
10. Itano, W.M. Perspectives on the quantum Zeno paradox. *J. Phys.* **2009**, *196*, 012018. [CrossRef]
11. Peres, A. Zeno paradox in quantum theory. *Am. J. Phys.* **1980**, *48*, 931–932. [CrossRef]
12. Zurek, W.H. Reversibility and stability of information processing systems. *Phys. Rev. Lett.* **1984**, *53*, 391–394. [CrossRef]
13. Franson, J.D.; Jacobs, B.C.; Pittman, T.B. Quantum computation using photons and the Zeno effect. *Phys. Rev. A* **2004**, *70*, 062302. [CrossRef]
14. Wang, X.B.; You, J.Q.; Nori, F. Quantum entanglement via two-qubit Zeno dynamics. *Phys. Rev. A* **2008**, *77*, 062339. [CrossRef]
15. Barontini, G.; Hohmann, L.; Hass, F.; Esteve, J.; Reichel, J. Deterministic generation of multiparticle entanglement by quantum Zeno dynamics. *Science* **2015**, *349*, 1317–1321. [CrossRef] [PubMed]
16. Nakanishi, T.; Yamane, K.; Kitano, M. Absorption-free optical control of spin systems: The quantum Zeno effect in optical pumping. *Phys. Rev. A* **2001**, *65*, 013404. [CrossRef]
17. Facchi, P.; Hradil, Z.; Krenn, G.; Pasczio, S.; Rehacek, J. Quantum Zeno tomography. *Phys. Rev. A* **2002**, *66*, 012110. [CrossRef]
18. Lepennen, N.V.; Lanco, L.; Smirnov, D.S. Quantum Zeno effect and quantum nondemolition spin measurement in quantum dot-micropillar cavity in the strong coupling regime. *Phys. Rev. B* **2021**, *103*, 045413. [CrossRef]
19. Minev, Z.K.; Mundhada, S.O.; Shankar, S.; Reinhold, P.; Gutierrez-Jaúregui, R.; Schoelkopf, R.J.; Mirrahimi, M.; Carmichael, H.J.; Devoret, M.H. To catch and reverse a quantum jump mid-flight. *Nature* **2019**, *570*, 200–204. [CrossRef]
20. Snizhko, K.; Kumar, P.; Romito, A. Quantum Zeno effect appears in stages. *Phys. Rev. Res.* **2020**, *2*, 033512. [CrossRef]
21. Meystre, P.; Sargent, M. *Elements of Quantum Optics*; Springer: Berlin/Heidelberg, Germany, 2007

22. Brewer, L.R.; Prestage, J.D.; Bollinger, J.J.; Itano, W.M.; Larson, D.J.; Wineland, D.J. Static properties of a non-neutral 9Be+ ion plasma. *Phys. Rev. A* **1988**, *38*, 859. [CrossRef]
23. Gerry, C.; Knight, P. *Introductory Quantum Optics*; Cambridge University Press: Cambridge, UK, 2005.
24. Ekert, A.; Knight, P. Entangled quantum systems and the Schmidt decomposition. *Am. J. Phys.* **1995**, *63*, 415–423. [CrossRef]
25. Zheng, W.; Xu, D.Z.; Peng, X.; Zhou, X.; Du, J.; Sun, C.P. Experimental demonstration of the quantum Zeno effect in NMR with entangled-based measurements. *Phys. Rev. A* **2013**, *87*, 032112. [CrossRef]